JOURNAL OF BACTERIOLOGY, Dec. 2005, p. 8047–8054 Vol. 187, No. 23
0021-9193/05/$08.00+0 doi:10.1128/JB.187.23.8047–8054.2005

Fine Structure of the *Deinococcus radiodurans* Nucleoid Revealed by Cryoelectron Microscopy of Vitreous Sections

Mikhail Eltsov* and Jacques Dubochet

Laboratoire d'Analyse Ultrastructurale, Bâtiment de Biologie, Université de Lausanne, CH-1015 Lausanne, Switzerland

Received 7 July 2005/Accepted 26 August 2005

Transmission electron microscopy revealed that the nucleoid of the extremely radioresistant bacteria *Deinococcus radiodurans* may adopt an unusual ring shape. This led to the hypothesis that the tight toroidal package of the *D. radiodurans* genome might contribute to radioresistance by preventing diffusion of ends of double-stranded DNA breaks. The molecular arrangement of DNA in the nucleoid, which must be determined to test this hypothesis, is not discernible by conventional methods of electron microscopy. We have applied cryoelectron microscopy of vitreous sections and found that the DNA arrangement in *D. radiodurans* differs from toroidal spooling. Diffuse coralline nucleoids of exponentially growing *D. radiodurans* do not reveal any particular molecular order. Electron-dense granules are generally observed in the centers of nucleoids. In stationary-phase cells, the nucleoid segregates from cytoplasm and DNA filaments show locally parallel arrangements, with increasing aspects of cholesteric liquid crystalline phase upon prolonged starvation. The relevance of the observed nucleoid organization to the radiation resistance of *D. radiodurans* is discussed.

Deinococcus radiodurans is a gram-positive, nonsporulating bacterium which usually grows in tetrad form. This organism is interesting because of its extreme resistance to DNA damage induced by ionizing radiation (4). It exhibits detectable survival after irradiation of 15,000 Gy (4) and grows continuously at 60 Gy/h (25). The unusual radiation resistance of *D. radiodurans* results from its ability to repair the genome, containing more than a hundred double-stranded DNA breaks, without mutations and loss of genome integrity (4, 32). The double-stranded DNA break repair in *D. radiodurans* is *recA*-dependent (10), but an explanation for its remarkable efficiency is yet to be found.

Initial analysis of *D. radiodurans* by transmission electron microscopy was performed in the 1970s (39, 40). Analysis focused mainly on the structure of the cell wall, in which a periodic S layer was described and characterized in detail (5, 38, 40). Methods available at that time did not reveal an unusual structure which could contribute to the radioresistance of *D. radiodurans*.

Interest in the organization of *D. radiodurans* has reawakened with recent advances in transmission electron microscopy techniques. Levin-Zaidman et al. (29). applied rapid freezing and freeze-substitution for their study of *D. radiodurans* nucleoids. They found that its nucleoid adopts an unusual ring shape. It is known that in vitro DNA tends to form toroidal aggregates in the presence of condensing agents (21). In these toroids, DNA molecules are condensed in a closely packed hexagonal arrangement (20). Levin-Zaidman at al. assumed that the ring-shaped nucleoid of *D. radiodurans* has basically the same structure. The hypothesis has been made that the toroidal shape facilitates repair of the fragmented genome because its densely packed structure prevents double-stranded DNA break ends from diffusing (13, 29).

The molecular arrangement of the DNA in the *D. radiodurans* nucleoid must be determined in order to test this hypothesis. Conventional methods of electron microscopy do not reveal the arrangement of DNA in bacteria, even when rapid freezing and freeze-substitution study are used because the bacterial chromatin aggregates during dehydration in the organic solvents, which are necessary in such preparations (23). Obtaining the fine structure of bacterial chromatin requires that fully hydrated specimens be observed.

Cryoelectron microscopy of vitreous sections (CEMOVIS) enables transmission electron microscopy observation of fully hydrated biological material. This method relies on vitrification of biological samples by rapid cooling, similar to the technique used in freeze-substitution. Then, instead of replacing the solidified water with an organic solvent and embedding the specimen in resin, native, unstained vitreous samples are cut at −140°C into thin sections which are observed in a cryoelectron microscope at even lower temperatures (2). CEMOVIS has been successfully applied to different biological samples, including bacteria. A number of new structural details not preserved by other methods of electron microscopy have been visualized in the cell envelope and extracellular matrixes of bacteria (3, 30, 31).

Single isolated DNA molecules can be visualized in a thin layer of vitreous water (12), but tracing DNA inside the crowded environment of a living cell remains a challenging task even if the structure is perfectly preserved by vitrification. Only when the DNA filaments are ordered and favorably oriented it is possible to determine their arrangement. CEMOVIS resolved the local DNA package in human and horse spermatozoa (36). It therefore seems probable that, if there is an ordered DNA package in *D. radiodurans*, it should be revealed in vitreous sections.

In this study we used CEMOVIS to examine the structure

* Corresponding author. Mailing address: Laboratoire d'Analyse Ultrastructurale, Bâtiment de Biologie, Université de Lausanne, CH-1015 Lausanne, Switzerland. Phone: 41 21 6924289. Fax: 41 21 6924285. E-mail: Mikhail.Eltsov@unil.ch.

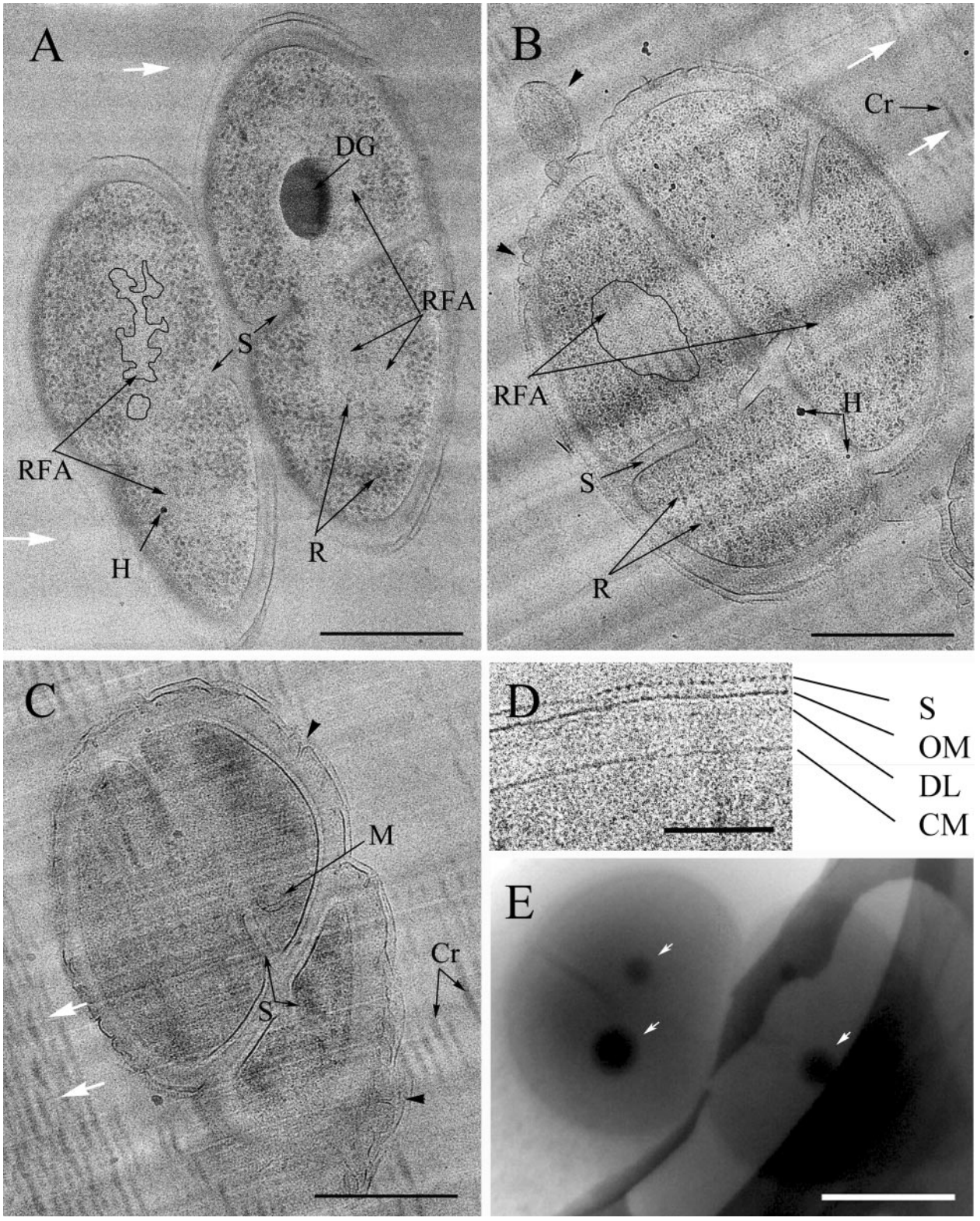

FIG. 1. (A, B, C) Vitreous sections of typical *D*. radiodurans tetrads from exponentially growing (A), stationary-phase (B), and long-stationary-phase (C) cultures were imaged with high defocus (5 to 10 μm) to obtain strong contrast favorable for general morphology mapping. Knife marks (white arrows) and crevasses (Cr) are cutting artifacts. H, surface contamination with hexagonal ice. The cytoplasm of some adjacent cells in the tetrad is interconnected through incomplete septa (S). A large electron-dense granule (DG) is visible inside the exponentially growing cell. The small granules are ribosomes (R). In the central part of the exponentially growing and stationary-phase cells, ribosome-free areas (RFA) are seen and are outlined in one cell of the tetrad. Note the dispersed coralline shape of the ribosome-free areas in exponentially growing cells (A) and the compact roundish shape in stationary-phase cells (B). Some membranous structures (M) are the only distinguishable structures in the highly dense

of nucleoids in exponentially growing and stationary-phase *D. radiodurans*. We found that nucleoids of exponentially growing bacteria have diffuse coralline shapes and do not show a visible molecular order. Electron-dense granules are generally observed in the center of nucleoids. In stationary-phase cells, the nucleoid segregates from the cytoplasm and DNA filaments show locally parallel arrangements, with increasing aspects of cholesteric liquid crystalline phase upon prolonged starvation. The possible relevance of the observed nucleoid organization to the radiation resistance of *D. radiodurans* and to the hypothesis of Levin-Zaidman et al. will be discussed.

MATERIALS AND METHODS

D. radiodurans strain SARK was grown in TGY broth (0.8% Bacto tryptone, 0.1% glucose, 0.4% yeast extract) at 30°C with vigorous shaking. Exponentially growing bacteria were collected after 10 to 12 h of growth at an optical density at 600 nm of 0.4 to 0.6. Stationary-phase and long-stationary-phase bacteria were collected after 4 days and 12 days of incubation, respectively. Bacteria were harvested by centrifugation with a Sorvall RS28S centrifuge for 5 min at 3,000 rpm. A soft pellet of bacteria was suspended with the same volume of 30% dextran (42 kDa, Sigma-Aldrich, St. Louis, MO), mixed by pipetting, and high-pressure frozen within 5 min in a Leica EMPACT (Leica, Vienna, Austria) apparatus. Thin frozen hydrated sections were obtained with a diamond cryoknife (Diatome, Biel, Switzerland) in a Leica FCS Ultracut S cryomicrotome with a nominal cutting feed of 50 nm at −140°C as described previously (3). For plunge freezing, 5 μl of bacterial suspension was placed on a holey carbon grid and frozen by plunging into liquid ethane, as described (1).

Grids containing thin frozen-hydrated sections or vitrified thin layers were mounted in a Gatan 626 cryospecimen holder (Gatan, Warrendale, PA) and observed below −180°C in Philips CM12 and CM100 cryoelectron microscopes (FEI, Eindhoven, The Netherlands) operating at an acceleration voltage of 80 kV. Electron micrographs were recorded on Kodak SO-136 electron image films or a 1K Multiscan charge-coupled device camera (Gatan, Warrendale, PA) or 2K TemCam charge-coupled device camera (TVIPS GmbH, Gauting, Germany). Negatives were digitalized using an Imacon Flextight Precision III scanner (Imacon, Redmond, WA). The contrast of micrographs was adjusted with Adobe Photoshop. No other image correction was performed. Fourier transforms of images were made with the Image J program (National Institutes of Health [http://rsb.info.nih.gov/ij/]).

RESULTS

General morphology of *D. radiodurans*. The cell morphology of *D. radiodurans* was checked immediately before vitrification by phase-contrast light microscopy. In all cultures *D. radiodurans* cells were observed mainly in tetrads, but diplococci were also seen occasionally.

D. radiodurans was well visible in vitreous sections. Figure 1 shows typical tetrads from exponentially growing (A), stationary-phase (B), and long-stationary-phase (C) cultures. The cytoplasm of the adjacent cells in the tetrad was either separated or interconnected through incomplete septa. Cutting artifacts such as compression, knife marks (white arrows), and crevasses are seen in the sections. Compression appears as a shortening of cell dimensions along the direction of cutting, resulting in the elliptical shape of the bacteria. The cutting direction is revealed by series of knife marks (Fig. 1A, B, and C, white arrows), which are irregularities in the thickness of sections originating from unevenness of the cutting edge of the knife. Crevasses are fissures perpendicular to the cutting direction. These cutting-induced artifacts are still frequent in vitreous sections (3) and must be considered during the interpretation of images.

A cell envelope is clearly visible around *D. radiodurans* cells. In regions of favorable orientation three sharp, high-contrast layers and one diffuse dense layer are visible in the cell envelope (Fig. 1A, B, and C). Such organization of the cell envelope is observed in all types of cultures. Figure 1D shows a magnified fragment of the cell envelope. The innermost sharp layer is the cytoplasmic membrane, while the intermediate one is the outer membrane. The outermost layer is the S-layer in which a periodic organization is seen on cross-sections and a hexagonal order on tangential sections (not shown). The diffuse dense layer is seen in the periplasmic space. It is most pronounced in long-stationary-phase cells. The outer membrane and the S-layer surround the entire tetrad and do not enter the septa. Irregularities in the structure of the outer part of the cell envelope, appearing as bubbles and wrinkles of the outer membrane and S-layer, are often observed in vitreous sections (Fig. 1C, black arrowheads).

Internal organization of cells differs in exponentially growing, stationary-phase, and long-stationary-phase cells. Multiple small granules and one or several large electron-dense granules are visible inside exponentially growing cells (Fig. 1A). The small granules are identified as ribosomes from their characteristic size and appearance. Ribosomes are distributed unevenly within the cell volume. The highest concentration of ribosomes is seen at the cell periphery. In the central part of the cell, individual ribosomes or small groups of ribosomes are spaced by ribosome-free areas. In a majority of exponentially growing cells these ribosome-free areas have a dispersed coralline shape (Fig. 1A, outlined).

Electron-dense granules are located in the central part of exponentially growing cells. Electron-dense granules have an elliptical shape in vitreous sections (Fig. 1A, dg). The large diameter of electron-dense granules rarely exceeds 400 nm. The small diameter of the ellipse is oriented along the cutting direction. This suggests that electron-dense granules are spherical bodies deformed into an elliptical shape by cutting-induced compression. In order to check whether electron-dense granules are an artifact of incubation with the cryoprotector, we performed plunge-freezing of whole-mount bacteria directly in culture medium. The thickness of the bacteria frozen in vitreous thin layers is too large for high-resolution imaging with a normal-voltage microscope, but due to their high electron density, electron-dense granules are nevertheless well visible (Fig. 1E, white arrows). This proves that electron-dense granules are a natural component of exponentially growing cells.

content of long-stationary-phase cells (C) in these imaging conditions. Irregularities in the structure of the outer part of the cell envelope (black arrowheads) are often observed in vitreous sections. (D) Magnified fragment of the cell envelope. The cytoplasmic membrane (CM), the diffuse dense layer (DL), the outer membrane (OM), and the outermost periodic S-layer (S) of the cell wall are distinguishable in vitreous sections. (E) Whole-mount exponentially growing tetrad plunge-frozen in culture medium. Note electron-dense granules (white arrows). Scale bars: A, B, and C, 500 nm; D, 100 nm; E, 1 μm.

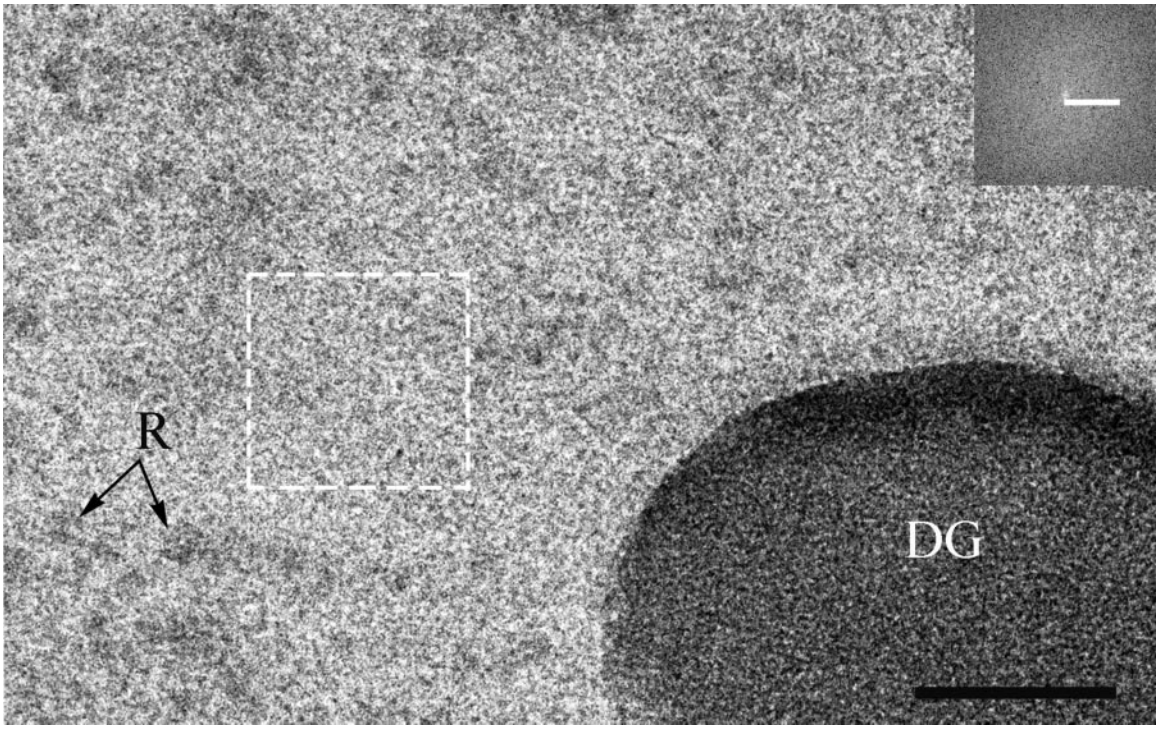

FIG. 2. High-resolution view of the central part of an exponentially growing cell (defocus, 1.8 μm). Electron-dense granule (DG), ribosomes (R), and other granules are visible. The space between the granules is disordered. Inset: Fourier transform of the outlined region. Scale bars: image, 100 nm; Fourier transform, $(5\ nm)^{-1}$.

Vitreous biological material is prone to beam damage. Irradiation with the electron beam changes the structure of the biological material. The ultimate state of damage is apparent as bubbling. We found that electron-dense granules begin to bubble simultaneously or soon after cell membranes, whereas ribosome-free areas are the most bubbling-resistant regions of cells.

In typical stationary-phase cells (Fig. 1B) electron-dense granules are not observed and ribosomes are excluded from the central part of the cells, forming large unified ribosome-free areas. These ribosome-free areas have a roundish shape and homogenous contents. Ribosome-free areas in adjacent stationary-phase cells can be interconnected (Fig. 1B).

On a few occasions, in both exponentially growing and stationary-phase cells, we found ring-shaped ribosome-free areas with an island of ribosome-rich cytoplasm in the center.

The content of a typical long-stationary-phase cell (Fig. 1C) has a high electron density, which makes it difficult to identify the internal components. Ribosomes and electron-dense granules are not distinguishable in long-stationary-phase cells. Occasionally some membranous structures are seen inside long-stationary-phase cells.

Interestingly, the bacterial populations in stationary-phase and long-stationary-phase cultures are not completely uniform. About 1% of the cells in a stationary-phase culture and few cells in a long-stationary-phase culture present aspects typical of exponentially growing cells; diffuse ribosome-free areas and electron-dense granules.

Fine structure of the nucleoid seen on vitreous sections. It is known from studies of freeze-substituted bacteria stained with osmium amine (19) that the bacterial nucleoid is located in ribosome-free areas. Hence, the ribosome-free regions visible in vitreous sections of exponentially growing and stationary-phase cells of *D. radiodurans* can be identified with the nucleoid.

Contrary to what happens in stained embedded specimens, the average density of the various regions of *D. radiodurans* is about the same everywhere, except in the dense granules. Imaging conditions favoring phase contrast over large areas must be used in order to obtain a significant contrast between the nucleoid and the rest of the bacteria.

Such conditions, implying high defocus (5 to 10 μm), have been used for recording Fig. 1 A to C. They are, however, not adequate for high-resolution observations. In order to reveal the molecular arrangement of the DNA in the nucleoid, a defocus compatible with the expected distances of few nanometers has been used (<3 μm).

Exponentially growing cells. Figure 2 shows a high-resolution view of the central region of an exponentially growing cell. Electron-dense granules are recognized because of the high contrast. As well as electron-dense granules, ribosomes and other granules, which can be transcription or replication complexes, are visible. The space between granules is disordered, and Fourier transform of the image does not reveal any predominant distance (Fig. 2, inset). Together these results suggest a dispersed, actively transcribed nucleoid without ordered compaction.

Stationary-phase cells. At high resolution, compact, roughly circular ribosome-free areas of stationary-phase cells do not appear to be homogenous any more, and specific textures

become apparent in them (Fig. 3A). The "dotted" pattern (Fig. 3B) consists of highly contrasting dots and lines which are clustered and, in several cases, form regularly spaced arrays (Fig. 3B, underlined with white). The "stripy" pattern is formed from longer and partially parallel lines (Fig. 3C) with lower contrast than the dots in the dotted pattern. Figures 3D and 3E show an intermediate case between dotted and stripy patterns which simultaneously contains dots and short and longer lines.

The high contrast of the dots suggests an accumulation of density along most of the section with a thickness averaging 70 nm. The diameter of the dots is in the range of 2 to 2.5 nm. Taken together, these aspects are characteristic of a DNA fragment seen along the viewing direction (6, 27). The dotted pattern can only be seen as a bundle of locally parallel DNA filaments whose direction is perpendicular to the section plan. The stripy patterns confirm the local parallel orientation of the DNA. They appear when the bundle is tilted with respect to the viewing direction. The Fourier transform reveals no reinforced dimensions in the ribosome-rich area (cytoplasm, Fig. 3A, left inset), whereas distances corresponding to 4 to 6 nm are reinforced in the ribosome-free regions. This characteristic order is best seen in the dotted regions (maximum at ca. 4.8 nm; Fig. 3A, right inset) and in the stripy areas.

The regions with local order do not entirely occupy ribosome-free areas. The clusters of dots and lines are spaced by regions without definable structure (Fig. 3B, C, and D, asterisks). The aspects of the local order are less pronounced in some nucleoids (Fig. 3E).

Long-stationary-phase cells. The crowded interior of long-stationary-phase cells does not allow us to distinguish the ribosome-containing area from the ribosome-free area at low magnification. Nevertheless, the specific organization of the central region of the cell revealed at higher resolution is similar to the dotted-stripy pattern observed in stationary phase (Fig. 4). The lines are frequently organized in arches characteristic of a cholesteric arrangement (8). This suggests that the DNA in the nucleoids of long-stationary-phase cells has a higher degree of order than in stationary-phase cells. The Fourier transform shows that the average interfilament distance corresponds to 4 nm (Fig. 4, inset), which is slightly shorter than in stationary-phase cells.

DISCUSSION

CEMOVIS revealed aspects of *D. radiodurans* structure which are not resolved by conventional electron microscopy embedding and sectioning techniques. For example, the periodic structure and hexagonal order of the S-layer of the cell envelope are directly seen in vitreous sections, whereas they were previously observed only on biochemically isolated S-layers or on freeze-etched cells (5, 37, 38).

Another characteristic aspect of native *D. radiodurans* structure is the dense spherical granules (electron-dense granules). Recent structural studies did not report electron-dense granules (9, 29), although early freeze-etching studies described spherical structures reminiscent of electron-dense granules in their size and location (37). Thornley et al. also observed dense granules in resin sections on a few occasions, but their content was often lost during cutting (39). It seems, therefore, that electron-dense granules do exist in *D. radiodurans* but they are optimally preserved only in frozen-hydrated material.

Electron-dense granules are located in the central part of exponentially growing bacteria in the nucleoid region. This addresses a question about the possible chromatin nature of electron-dense granule. However, their high sensitivity to beam-induced bubbling suggests that they do not have a high nucleic acid concentration, since aromatic-rich materials are radiation resistant (11). Due to structural similarity, Thornley et al. (39) associated electron-dense granules with polyphosphate granules observed in other species of bacteria. Phosphate, in combination with proteins, would account for the high density and radiation sensitivity of the granules. The precise composition of electron-dense granules, however, remains to be identified.

CEMOVIS successfully revealed aspects of the molecular arrangement of DNA within *D. radiodurans* nucleoids. The diffuse coralline nucleoids of exponentially growing cells do not show any particular order. We attribute this to the high transcriptional and replication activity required for active growth. A local order first appears in stationary-phase cells in the form of bundles of locally parallel DNA filaments with an average interfilament distance of 4.8 nm. Upon prolonged starvation the aspect of cholesteric liquid crystalline order is observed and the average interfilament distance shortens to 4.0 nm. The gradual increase in the local order together with reduction of the interfilament distance suggests a liquid crystalline organization of the *D. radiodurans* nucleoid.

It is known that liquid crystalline phases of DNA spontaneously assemble in vitro with increasing DNA concentration (26). In bacteria, the increased DNA concentration leading to liquid crystallization may result from accumulation of high-copy plasmids (34), but this is not the case for stationary-phase cells of *D. radiodurans*, in which DNA content per cell is lower than in exponentially growing cells (18). Since at stationary phase the nucleoid segregates to a compact round domain excluding ribosomes, the crowding of DNA can be originated by its redistribution into the confined part of the cell volume. This effect can be related to the fact that cholesteric liquid crystalline nucleoids were found in starving *Escherichia coli* lacking Dps, an abundant starvation-induced unspecific DNA binding protein (16). In contrast, wild-type *E. coli* and strains overexpressing Dps show nucleoid compaction by formation of DNA-Dps cocrystals with a specific structural appearance different from that observed in *D. radiodurans* (15, 16). It can therefore be concluded that the segregation and compaction of the *D. radiodurans* nucleoid can be driven by a decrease of protein-DNA binding in the stationary phase. In addition, an unusually high concentration of Mn^{2+} ions found in *D. radiodurans* (9, 28) can facilitate liquid crystalline compaction by compensating for repulsive forces between DNA molecules.

A minority of cells in stationary-phase cultures of *D. radiodurans* have the typical morphology of exponentially growing cells. We attribute this morphological polymorphism to the presence of mutants gaining a growth advantage during the extended stationary phase (14).

Nucleoid shapes that can be interpreted as rings have been found in only a few cases. This observation argues against the results of other researchers showing an abundance of ring-like nucleoids, which were considered DNA toroids (29). We sus-

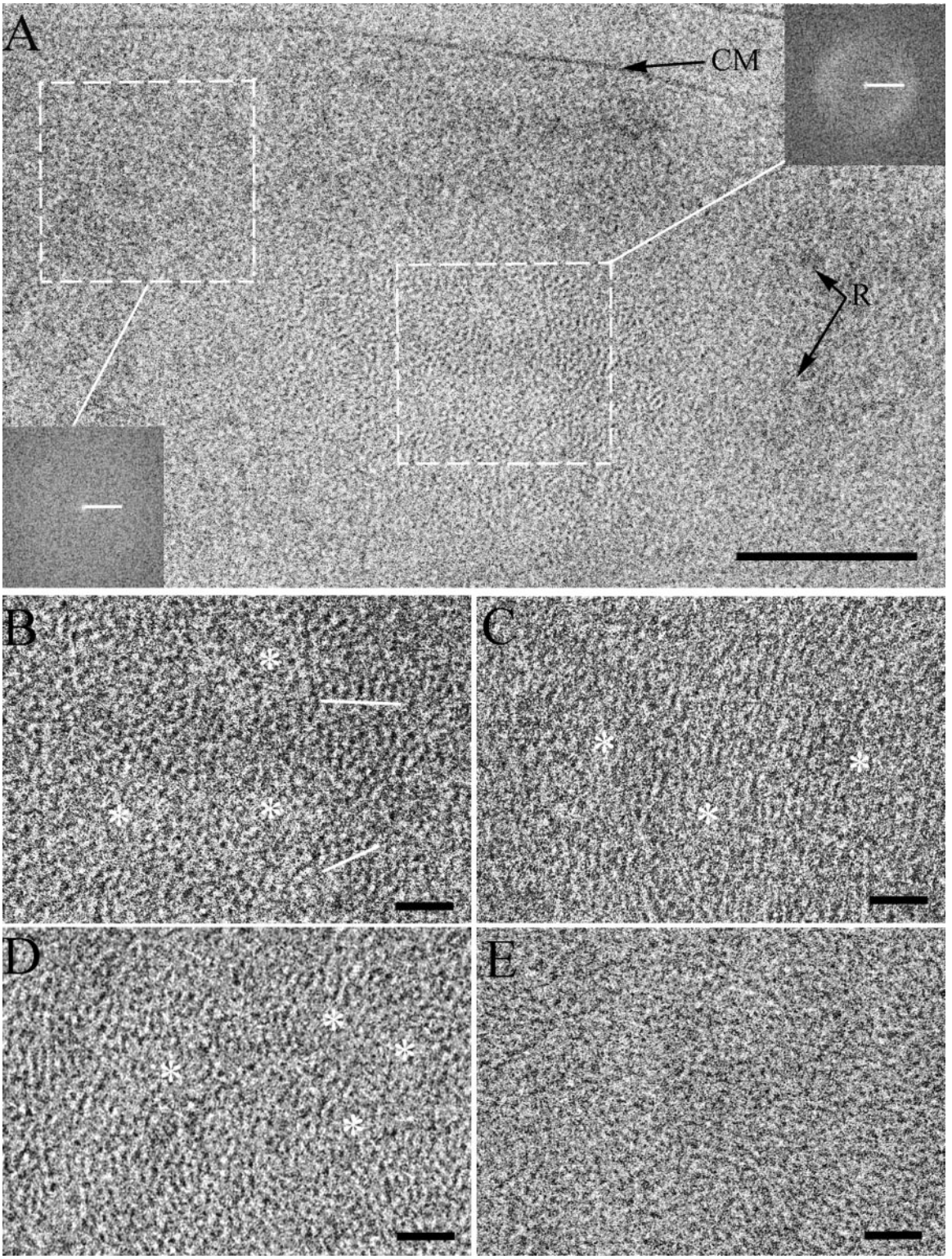

FIG. 3. Fine structure of the nucleoid in stationary-phase cells. A, High-resolution view of stationary-phase cell (defocus, 2 μm). At this defocus the contrast of ribosomes (R) is faded, but fine structural details are visible in the nucleoid. Insets show Fourier transforms of the corresponding marked regions of the cell. CM, cytoplasmic membrane. B, C, D, and E, Different structural textures of the nucleoid. B, Dotted pattern. Regularly spaced arrays of dots are underlined in white. C, Stripy pattern. D and E, Intermediate case between dotted and stripy patterns which simultaneously contains dots and short and longer lines. The clusters of dots and lines are spaced by the regions without definable structure (asterisks). The aspects of the local order are less pronounced in some nucleoids (E). Scale bars: A, 100 nm; B, C, D, and E, 20 nm; Fourier transforms, $(5\ \text{nm})^{-1}$.

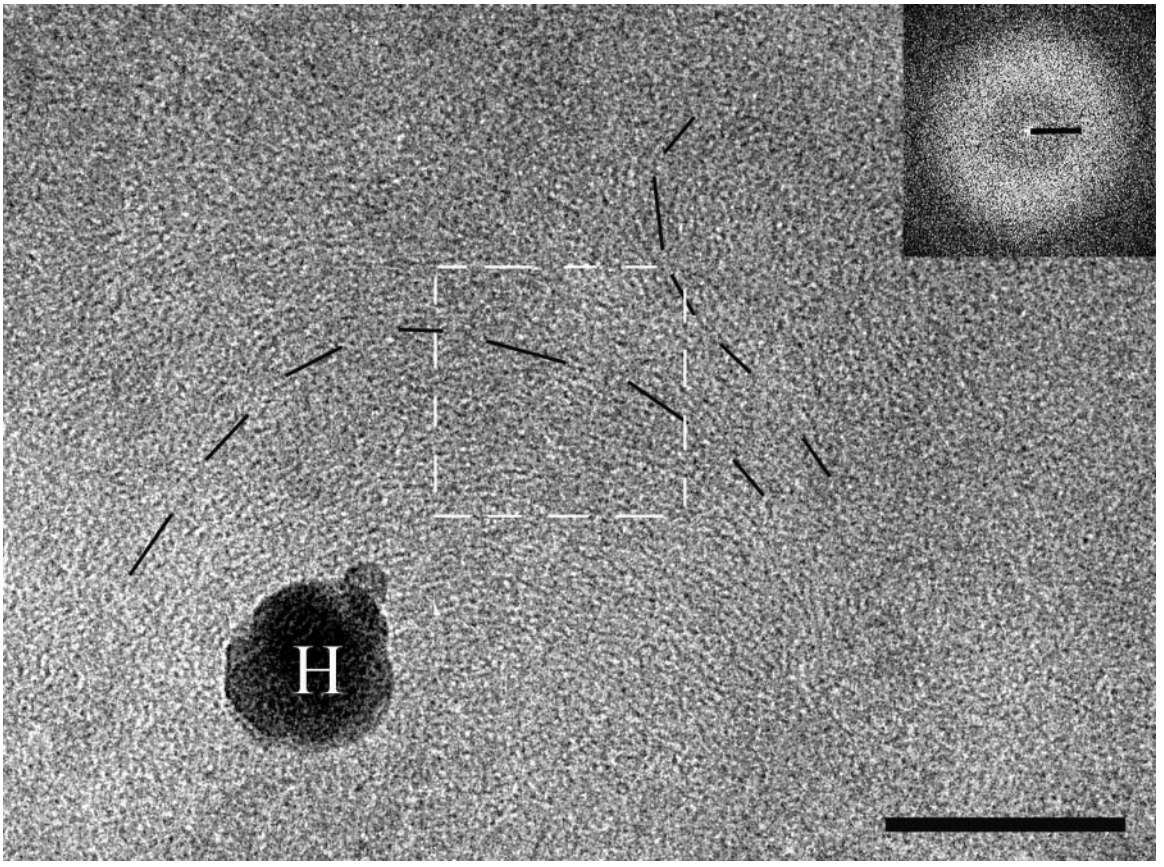

FIG. 4. Nucleoid of long-stationary-phase cells shows the aspect of cholesteric arrangement: arches (dashed lines) formed by dots and lines (defocus, 1.6 μm). H, surface contamination with hexagonal ice. Inset: Fourier transform of the marked region. Scale bars: image, 100 nm; Fourier transform, $(5\ \text{nm})^{-1}$.

pect that conventional studies have misinterpreted the dispersed nucleoids as DNA toroids when the central electron-dense granule is lost during sample preparation and the resolution is insufficient to define the molecular arrangement. Our high-resolution analysis reveals that the DNA arrangement in nucleoids of *D. radiodurans* differs from toroidal DNA spooling both in actively growing and in stationary-phase cultures.

Diffuse coralline nucleoids without a specific molecular order observed in exponentially growing *D. radiodurans* are similar to those of nonradioresistant bacteria (7, 19, 30). Nevertheless, exponentially growing cells of *D. radiodurans* are known to tolerate 5,000 Gy (33). Stationary-phase cultures have a radioresistance approximately three times higher, but this increase already occurs at the beginning of the stationary-phase (24) and is therefore independent of the ordered genome compaction which appears with the aging of the culture. This suggests that the arrangement of the nucleoid does not play a key role in the radioresistance of *D. radiodurans*. Even if it does, the mechanism must differ from the one proposed by Levin-Zaidman et al. (29), in which the dense toroidal package prevents separation of double-stranded DNA break ends, thus favoring efficient repair.

We have found that the dense toroidal package probably does not exist in *D. radiodurans*. Furthermore, we observed that the ordered condensation of DNA, leading to cholesteric organization, always remains changing and dynamic. It might well be that the diffusibility of DNA fragments is reduced in liquid crystals but that is the nature of this type of order; they still remain mobile. This is confirmed by experiments in λ phage DNA cyclization in the presence of polyamines, which show that DNA ends remains mobile in most condensed liquid crystalline phases (22). The hypothesis that the liquid crystalline order of DNA is not directly related to radioresistance is also supported by the fact that dinoflagellata, whose genome is normally in the form of cholesteric liquid crystal (35), are not unusually radioresistant.

The fact that the segregation of the nucleoid from the ribosome-rich cytoplasm is already complete at the early phase of DNA ordering suggests that nucleoid separation is the basic structural change accompanying the transition to the stationary phase. Therefore it could be relevant to the increase in radioresistance at the beginning of stationary phase. This idea is supported by fact that the nucleoids of radiation-sensitive bacteria remain coralline and dispersed at stationary phase (17, 41), whereas the nucleoids of radioresistant bacterial species are more localized (41). We speculate that the segregation of nucleoids reduces the damage caused by free radicals generated in the cytoplasm by radiation (17).

The molecular arrangement of DNA revealed in the nucle-

oid of *D. radiodurans* cannot directly serve as a structural support for DNA repair. We believe that the unusual efficiency of the latter in *D. radiodurans* is more likely to have a physiological than a structural basis. Nevertheless, nucleoid segregation at the stationary phase can be protective and requires further study.

ACKNOWLEDGMENTS

This work was supported by the 3D-EM Network of Excellence within Research Framework Programme 6 of the European Commission.

We are grateful to H. Engelhardt for supplying bacteria and to A. Minsky for stimulating discussions.

REFERENCES

1. **Adrian, M., J. Dubochet, J. Lepault, and A. W. McDowall.** 1984. Cryo-electron microscopy of viruses. Nature **308:**32–36.
2. **Al-Amoudi, A., J. J. Chang, A. Leforestier, A. McDowall, L. M. Salamin, L. P. Norlen, K. Richter, N. S. Blanc, D. Studer, and J. Dubochet.** 2004. Cryo-electron microscopy of vitreous sections. EMBO J. **23:**3583–3588.
3. **Al-Amoudi, A., L. P. Norlen, and J. Dubochet.** 2004. Cryo-electron microscopy of vitreous sections of native biological cells and tissues. J. Struct. Biol. **148:**131–135.
4. **Battista, J. R.** 1997. Against all odds: the survival strategies of *Deinococcus radiodurans*. Annu. Rev. Microbiol. **51:**203–224.
5. **Baumeister, W., M. Barth, R. Hegerl, R. Guckenberger, M. Hahn, and W. O. Saxton.** 1986. Three-dimensional structure of the regular surface layer (HPI layer) of *Deinococcus radiodurans*. J. Mol. Biol. **187:**241–250.
6. **Bednar, J., P. Furrer, A. Stasiak, J. Dubochet, E. H. Egelman, and A. D. Bates.** 1994. The twist, writhe and overall shape of supercoiled DNA change during counterion-induced transition from a loosely to a tightly interwound superhelix. Possible implications for DNA structure in vivo. J. Mol. Biol. **235:**825–847.
7. **Bohrmann, B., W. Villiger, R. Johansen, and E. Kellenberger.** 1991. Coralline shape of the bacterial nucleoid after cryofixation. J. Bacteriol. **173:**3149–3158.
8. **Bouligand, Y.** 1978. Liquid crystalline order in biological materials, p 261–297. *In* A. Blumstein (ed.), Liquid crystalline order in polymers. Academic Press, New York, N.Y.
9. **Daly, M. J., E. K. Gaidamakova, V. Y. Matrosova, A. Vasilenko, M. Zhai, A. Venkateswaran, M. Hess, M. V. Omelchenko, H. M. Kostandarithes, K. S. Makarova, L. P. Wackett, J. K. Fredrickson, and D. Ghosal.** 2004. Accumulation of Mn(II) in *Deinococcus radiodurans* facilitates gamma-radiation resistance. Science **306:**1025–1028.
10. **Daly, M. J., and K. W. Minton.** 1997. Recombination between a resident plasmid and the chromosome following irradiation of the radioresistant bacterium *Deinococcus radiodurans*. Gene **187:**225–229.
11. **Dubochet, J.** 1975. Carbon loss during irradiation of T4 bacteriophages and *E. coli* bacteria in electron microscopes. J. Ultrastruct. Res. **52:**276–288.
12. **Dubochet, J., J. Bednar, P. Furrer, A. Z. Stasiak, A. Stasiak, and A. A. Bolshoy.** 1994. Determination of the DNA helical repeat by cryo-electron microscopy. Nat. Struct. Biol. **1:**361–363.
13. **Englander, J., E. Klein, V. Brumfeld, A. K. Sharma, A. J. Doherty, and A. Minsky.** 2004. DNA toroids: framework for DNA repair in *Deinococcus radiodurans* and in germinating bacterial spores. J. Bacteriol. **186:**5973–5977.
14. **Finkel, S. E., and R. Kolter.** 1999. Evolution of microbial diversity during prolonged starvation. Proc. Natl. Acad. Sci. USA **96:**4023–4027.
15. **Frenkiel-Krispin, D., I. Ben-Avraham, J. Englander, E. Shimoni, S. G. Wolf, and A. Minsky.** 2004. Nucleoid restructuring in stationary-state bacteria. Mol. Microbiol. **51:**395–405.
16. **Frenkiel-Krispin, D., S. Levin-Zaidman, E. Shimoni, S. G. Wolf, E. J. Wachtel, T. Arad, S. E. Finkel, R. Kolter, and A. Minsky.** 2001. Regulated phase transitions of bacterial chromatin: a non-enzymatic pathway for generic DNA protection. EMBO J. **20:**1184–1191.
17. **Ghosal, D., M. V. Omelchenko, E. K. Gaidamakova, V. Y. Matrosova, A. Vasilenko, A. Venkateswaran, M. Zhai, H. M. Kostandarithes, H. Brim, and K. S. Makarova.** 2005. How radiation kills cells: Survival of *Deinococcus radiodurans* and *Shewanella oneidensis* under oxidative stress. FEMS Microbiol. Rev. **29:**361–375.
18. **Hansen, M. T.** 1978. Multiplicity of genome equivalents in the radiation-resistant bacterium *Micrococcus radiodurans*. J. Bacteriol. **134:**71–75.
19. **Hobot, J. A., W. Villiger, J. Escaig, M. Maeder, A. Ryter, and E. Kellenberger.** 1985. Shape and fine structure of nucleoids observed on sections of ultrarapidly frozen and cryosubstituted bacteria. J. Bacteriol. **162:**960–971.
20. **Hud, N. V., and K. H. Downing.** 2001. Cryoelectron microscopy of lambda phage DNA condensates in vitreous ice: The fine structure of DNA toroids. Proc. Natl. Acad. Sci. USA **98:**14925–14930.
21. **Hud, N. V., and I. D. Vilfan.** 2005. Toroidal DNA condensates: unraveling the fine structure and the role of nucleation in determining Size. Annu. Rev. Biophys. Biomol. Struct. **34:**295–318.
22. **Jary, D., and J. L. Sikorav.** 1999. Cyclization of globular DNA. Implications for DNA-DNA interactions in vivo. Biochemistry **38:**3223–3227.
23. **Kellenberger, E., and B. Arnold-Schulz-Gahmen.** 1992. Chromatins of low-protein content: special features of their compaction and condensation. FEMS Microbiol. Lett. **79:**361–370.
24. **Keller, L. C., and R. B. Maxcy.** 1984. Effect of physiological age on radiation resistance of some bacteria that are highly radiation resistant. Appl. Environ. Microbiol. **47:**915–918.
25. **Lange, C. C., L. P. Wackett, K. W. Minton, and M. J. Daly.** 1998. Engineering a recombinant *Deinococcus radiodurans* for organopollutant degradation in radioactive mixed waste environments. Nat. Biotechnol. **16:**929–933.
26. **Leforestier, A., and F. Livolant.** 1993. Supramolecular ordering of DNA in the cholesteric liquid crystalline phase: an ultrastructural study. Biophys. J. **65:**56–72.
27. **Leforestier, A., H. U. Nissen, and J. Dubochet.** 1995. DNA-DNA interaction in thin layer analysed by cryo-electron microscopy. C. R. Acad. Sci. Ser. III Sci. Vie **318:**1015–1020.
28. **Leibowitz, P. J., L. S. Schwartzberg, and A. K. Bruce.** 1976. The in vivo association of manganese with the chromosome of *Micrococcus radiodurans*. Photochem. Photobiol. **23:**45–50.
29. **Levin-Zaidman, S., J. Englander, E. Shimoni, A. K. Sharma, K. W. Minton, and A. Minsky.** 2003. Ringlike structure of the *Deinococcus radiodurans* genome: a key to radioresistance? Science **299:**254–256.
30. **Matias, V. R., A. Al-Amoudi, J. Dubochet, and T. J. Beveridge.** 2003. Cryo-transmission electron microscopy of frozen-hydrated sections of *Escherichia coli* and *Pseudomonas aeruginosa*. J. Bacteriol. **185:**6112–6118.
31. **Matias, V. R., and T. J. Beveridge.** 2005. Cryo-electron microscopy reveals native polymeric cell wall structure in *Bacillus subtilis* 168 and the existence of a periplasmic space. Mol. Microbiol. **56:**240–251.
32. **Minton, K. W., and M. J. Daly.** 1995. A model for repair of radiation-induced DNA double-strand breaks in the extreme radiophile *Deinococcus radiodurans*. Bioessays **17:**457–464.
33. **Moseley, B. E., and A. Mattingly.** 1971. Repair of irradiation transforming deoxyribonucleic acid in wild type and a radiation-sensitive mutant of *Micrococcus radiodurans*. J. Bacteriol. **105:**976–983.
34. **Reich, Z., E. J. Wachtel, and A. Minsky.** 1994. Liquid-crystalline mesophases of plasmid DNA in bacteria. Science **264:**1460–1463.
35. **Rill, R. L., F. Livolant, H. C. Aldrich, and M. W. Davidson.** 1989. Electron microscopy of liquid crystalline DNA: direct evidence for cholesteric-like organization of DNA in dinoflagellate chromosomes. Chromosoma **98:**280–286.
36. **Sartori Blanc, N., A. Senn, A. Leforestier, F. Livolant, and J. Dubochet.** 2001. DNA in human and stallion spermatozoa forms local hexagonal packing with twist and many defects. J. Struct. Biol. **134:**76–81.
37. **Sleytr, U. B., M. Kocur, A. M. Glauert, and M. J. Thornley.** 1973. A study by freeze-etching of the fine structure of *Micrococcus radiodurans*. Arch. Microbiol. **94:**77–87.
38. **Sleytr, U. B., M. T. Silva, M. Kocur, and N. F. Lewis.** 1976. The fine structure of *Micrococcus radiophilus* and *Micrococcus radioproteolyticus*. Arch. Microbiol. **107:**313–320.
39. **Thornley, M. J., R. W. Horne, and A. M. Glauert.** 1965. The fine structure of *Micrococcus radiodurans*. Arch. Mikrobiol. **51:**267–289.
40. **Work, E., and H. Griffiths.** 1968. Morphology and chemistry of cell walls of *Micrococcus radiodurans*. J. Bacteriol. **95:**641–657.
41. **Zimmerman, J. M., and J. R. Battista.** 2005. A ring-like nucleoid is not necessary for radioresistance in the *Deinococcaceae*. BMC Microbiol. **5:**17.